MONITORING AND ANALYSIS OF NYAMULAGIRA VOLCANO ACTIVITY USING MODIS DATA: CASE OF THE 2011-2012 ERUPTION

MONTFORT BAGALWA[a,b], KATCHO KARUME[a,b]

[a] *Department of Geodesy, Goma Volcano Observatory, Goma, North Kivu, D.R.Congo.*
e-mail: louisbagalwa@yahoo.fr
[b] *Université Evangélique en Afrique, Bukavu-South Kivu, Bukavu, D.R.Congo.*
e-mail: kkatcho@yahoo.com, Tél. : +243997738095 & +243994304633

Received: 16th March 2015, **Accepted:** 30th July 2015

ABSTRACT

In this paper we analyzed the 2011-2012 eruption of Nyamulagira volcano using MODIS Data. Eruptions have been occurring every 3–4 years throughout the last century. Satellite infrared data, collected by MODIS sensor to estimate pixels thermal anomaly of hot spots were analized, the radiance emitted at 3,959 and 12.02μm for each pixel and the thermal emissions at Nyamulagira feall into three distinct radiating regimes released during the 2011–2012 eruption. Initial activity was detected on 6 November, at 19:55 UTC, with a large thermal anomaly with 28 pixels approximately on the north flank of the volcano. The anomaly was limited to the north flank. The anomaly reached a maximum size of 1188 pixels in January 2012. The size and intensity of the anomaly rapidly diminished to first April 2012 were no more than 2 piixels indicate the end of eruption.

Keywords: Nyamuragira volcano, MODIS, Thermal anomalies, Pixel, Hot spot, Volcanic radiative power, Thermal regimes, Effusive trends.

INTRODUCTION

Virunga active Volcanoes are difficult to access due to the increasing insecurity in the volcanic Virunga region in general; forcing satellite surveillance. Together with other space-based techniques, thermal monitoring of volcanic activity has evolved rapidly over the past decade (Wright *et al*., 2004; Harris *et al.*, 2000a.). The launch of new satellites each year and new developments in remote sensing techniques have expanded the capability of scientists worldwide to monitor volcanoes using satellites. For the purpose of volcanic research, remote sensing is the detection of electromagnetic energy that is absorbed, reflected, radiated, or scattered from the surface of a volcano or from its erupted material during an eruption, sensed by satellites. In particular, the identification of thermal anomalies from space has numerous applications, including the detection of volcanic eruptions (Harris *et al*., 1997; Rothery *et al*., 2005).

The MODIS instrument (Moderate Resolution Imaging Spectroradiometer), aboard the Terra (EOS AM) and Aqua (EOS PM) satellites, offers a temporal coverage (~4 images-day^{-1}), spatial resolution (1 km in the IR bands) and an adequate spectral coverage (the "fire channel" at ~4 μm on MODIS band 21) to enable the detection and quantification of thermal emissions related to several types of volcanic activity

(Coppola *et al*., 2013; Wright *et al*. 2008a, 2004, 2002; Rothery *et al*. 2005). Although, MODIS has been used to quantify volumetric fluxes at basaltic volcanoes, such as Mount Etna (Steffke *et al*,. 2011; Harris *et al*., 2011), Stromboli (Ripepe *et al*., 2005; Calvari *et al*., 2010; Coppola *et al*., 2012), Piton de la Fournaise (Coppola *et al*., 2009, 2010; Gouhier & Coppola, 2011) and Kilauea (Di Bartola *et al.*, 2008; Koeppen *et al.*, 2013), its application in the analysis of Nyamuragira eruptions has addressed this issue only partially, with only qualitative observations (Wright & Pilger, 2008; Wadge & Burt, 2011).

In this paper, we used MODVOLC data recorded during the 2011-2012 eruption of Nyamulagira volcano. They were recorded between November 2011 and the last eruption on April 2012. The study evaluates the NTI remotely sensed index for mapping and analyzing of the Nyamulagira 2011-2012 eruption.

The study demonstrates the ability of the MODVOLC data for monitoring and detecting hotspots during the eruption of the Nyamulagira volcano.

Geological background and the recent eruption of Nyamulagira

The Nyamuragira volcano (3058 m) is located in the Virunga Volcanic Zone, a sector of the western branch of the East African Rift (Fig. 1), just north of Lake Kivu. Its total average volume is about 500 x 109 m3 and its position follows the east-west trend of the African Rift System (Pouclet, 1975). Nyamulagira is among the most dangerous volcanoes in the world for the risks associated with the spread of lava flows and pyroclastic materials. It is one of the most historically active volcanoes in the Virunga chain (Smets *et al.*, 2010) and in Africa, producing 38 eruptions since the beginning of the twentieth century (Wadge & Burt, 2011). The activity of Nyamulagira could be directly related to the opening of the West African rift (Hamaguchi & Zana, 1983). Since the 1940s, volcanic activity has been characterized by episodic flank effusive eruptions with intervals of summit lava lake activity (Hamaguchi & Zana, 1983). Most eruptions, with the exception of the 1938 summit eruption, occur on the flanks of the volcano, recent eruptions sides began on 27 January 2000, 05 February 2001, 25 July 2002, 08 May 2004, 27 November 2006 (Mavonga *et al*., 2010; Hayashi *et al*., 1992), 01 January 2010 and 06 November 2011. Eruptions are fed by dykes and fissures that occasionally cut the summit caldera (∼2km in diameter), and more often propagate down the flanks of the volcano (Wadge & Burt, 2011). Eruption onsets are characterized by the ejection of lava fountains that may reach 200–300 m in height, and may involve one or more fissure vents (Coppola & Cigolini, 2013). A transition from Hawaiian-type fountaining to Strombolian activity may eventually occur (Ueki, 1983; Burt *et al*., 1994). Due to the lack of field observations, the date of the end of the eruption is often uncertain (Coppola & Cigolini, 2013; Wadge & Burt, 2011).

Following the intense lava and gas production occurring during the early stages of eruption, lava effusion often diminishes gradually before ceasing (Coppola & Cigolini, 2013; Head *et al*,. 2012; Wadge & Burt, 2011; Bluth & Carn, 2008). The very low amplitude of the pre-eruptive inflation suggests that the vigorous lava fountaining and gas release, typical of this initial activity, is essentially driven by magma decompression rather than by the release of elastic energy stored in the wallrocks reservoir (Toombs & Wadge, 2012).

The volume of product of Nyamulagira in particular, has been calculated for each known eruption since 1901. The average throughput of magmatic activity is between 5 and 30 x 106 m3 per year. Nyamulagira is characterized by very potassic lavas, a volcanism with basic dominance with basanite leucifere, limburgite, leucite and nepheline, hyper-sodic and high-potassium; also including diverse products such as tholeiites; resulting of seven major volcanic devices among two are still active. This volcanic activity probably started in the

Pleistocene (Villeneuve, 1980). Nyamulagira lavas are alkali basalts, hawaiites, basanites and tephrites with SiO_2 ranging from 43 to 56 wt % (Aoki *et al*., 1985; Pouclet, 1975).

Recently, erupted products show a rather restricted compositional range with silica contents from 45.2 to 46.3 SiO_2 wt % (Chakrabarti *et al*., 2009; Head *et al.*, 2011).

The recent Nyamulagira eruption started on November 6, 2011 at 03:55, following 2 days of intense seismicity (Coppola & Cigolini, 2013; Smithsonian, 2011) and finished on 03 April 2012. Lava effusion occurred from a fissure located about 12 km ENE of the main crater with an orientation of ~N70°E. The first fracture opened in east-west orientation where the lava spilled out, forming fountains and lava flows (Coppola & Cigolini, 2013). The easting of 1989 Lava was partially covered by lava estimated at 252 (±126)mm^3 emplaced during the 2011–2012 flank eruption which made this event one of the most voluminous eruptions occurred at Nyamuragira volcano in the last century (Coppola & Cigolini, 2013; Wadge & Burt, 2011). Based on a Landsat ETM+ (Enhanced Thematic Mapper Plus) image collected on March 28, 2012, Coppola & Cigolini (2013) estimated that the final lava field had covered an area of ~26.8 km^2 with the maximum length of 11.3 km approximatively.

More than 1,500 km^2 were covered by lava flows up to about 30 km away (Smets *et al*., 2010). The lava flows and pyroclastic products of Nyamulagira can be considered as a less immediate threat to the public because of the distance from dwellings, their low speed and viscosity; but a real threat to the Virunga National Park and the surrounding population; a risk for its outstanding biodiversity. Nyamulagira erupts every two to four years and is also well known because of the tephra emissions (Smets *et al*., 2010).

Modis instrument and Modvolc algorithm.

The Moderate Resolution Imaging Spectroradiometer (MODIS) is a key instrument aboard the Terra (EOS AM) and Aqua (EOS PM) satellites MODIS which was launched into a sun-synchronous (10:30 AM equatorial crossing) polar orbit on board NASA's first EOS platform, Terra on December 18, 1999 (Wright *et al*., 2004). A second MODIS sensor was launched in April 2002 on the EOS platform"Aqua". Terra's orbit around the Earth is timed so that it passes from north to south across the equator in the morning, while Aqua passes south to north over the equator in the afternoon so they acquire 2 daytime images and 2 images per day (Wright *et al*., 2002). The MODIS instrument is a nadir viewing system having a swath width of 2,330 km and offering 36 spectral bands of data at one of 3 spatial resolutions of 250, 500, or 1,000 meters per pixel (Table 1), but summarized at http://ltpwww.gsfc.nasa.gov/MODIS/MODIS.html (Flynn *et al*., 2001). Ten of these 36 spectral bands are useful for detecting thermal radiance from active volcanic (Flynn *et al*., 2001). The MODIS have four MIR bands (20, 21, 22 and 23) centered around 3.75; 3.95 and 4.05μm, and three TIR bands (29, 31 and 32) centered around 8.55; 11.03 and 12.02μm used in different environments volcanic (Wright *et al*., 2004; Flynn *et al*., 2002; Wright *et al.*, 2002).

The MODIS Thermal Alerts Web site, developed and maintained by the Hawaii Institute of Geophysics and Planetology's MODIS Thermal Alert Team hosts the first truly global high-temperature thermal monitoring system (Wright *et al*., 2004; Flynn *et al*., 2002; Wright *et al.*, 2002). New MODIS data granules are received and processed by the Goddard DAAC every 5 minutes. Computer resources at the DAAC require the data to be processed in real-time in order to keep up with the data stream. MODIS night-time data granules do not have the 500 m in bands 5, 6, and 7 data which, using the ATSR example, have been shown to be excellent for characterizing high temperature objects at night (Flynn *et al.*, 2002; Wooster & Rothery, 2001).

Table 1: Summary of MODIS Spectral Bands (Flynn *et al.*, 2001)

Band	Bandwidth (nm)	Pixel size (m)
1	620 - 670	250
2	841 - 876	250
3	459 – 479	500
4	545 – 565	500
5	1230 – 1250	500
6	1628 – 1652	500
7	2105 – 2155	500
8	405 – 420	1000
9	438 – 448	1000
10	483 – 493	1000
11	526 – 536	1000
12	546 – 556	1000
13	662 – 672	1000
14	673 – 683	1000
15	743 – 753	1000
16	862 – 877	1000
17	890 – 920	1000
18	931 – 941	1000
19	915 – 965	1000
20	3660 – 3840	1000
21	3929 – 3989	1000
22	3929 – 3989	1000
23	4020 – 4080	1000
24	4433 – 4498	1000
25	4482 – 4549	1000
26	1360 – 1390	1000
27	6535 – 6895	1000
28	7175 – 7485	1000
29	8400 – 8700	1000
30	9580 – 9880	1000
31	10780 – 11280	1000
32	11770 – 12270	1000
33	13185 – 13485	1000
34	13485 – 13785	1000
35	13785 – 14085	1000
36	14085 – 14385	1000

The MODIS Thermal Alerts Web site provides a series of maps updated every 24 hours to show 'thermal alerts'. Originally, the Website showed only night-time alerts (approximately 22:30 local time for Terra and 02:30 for Aqua), but now it also shows daytime alerts at approximately 10:30 and 14:30 local time (Wright *et al*., 2004, 2002; Flynn *et al*., 2002). The MODIS thermal alert project was developed as an add-on through the EOS Volcanology Interdisciplinary Science Team effort. The MODIS thermal alert code had to be very simple and use only a few MODIS bands to achieve its objective. It had to run quickly and efficiently. MODIS thermal alert had to be embedded in the initial MODIS processing sequence so results could be reported in near real time (Flynn *et al*., 2002).

Wright *et al*. (2002) provide a full description of how the MODVOLC (MODIS Volcano alert) algorithm was developed, tested and implemented. The MODVOLC algorithm is a point operation which analyses the Level 1B MODIS radiance data from three wave-bands (21, 22, and 32) using four mathematical operations. Surfaces that are thermally homogenous at the pixel scale can be discriminated on the basis of differences in the amount of radiance they emit at 4 and 12 μm. The MODVOLC algorithm developed by the MODIS Alert team is

based on the fact that a sub-pixel hotspot causes the amount of radiance emitted at 4μm to increase at a much greater rate than at 12μm (Piscopo *et al*., 2008; Wright *et al*., 2004; Flynn *et al*., 2002; Wright *et al*., 2002).

However, this helps little in discriminating sub-pixel-sized volcanic hotspots, a consequence of the contrasting nature of the relationship between temperature and emitted radiance at 4 and 12 μm. By normalizing the difference between the recorded 4 and 12 μm radiance by the sum of the 4 and 12 μm radiances, an index can be obtained that is weighted against those surfaces that emit substantial levels of radiance at 4 μm (i.e. the lava flows) rather than those which emit lower amounts of radiance at this wavelength (i.e. the cold clouds). This is the basis of the Normalised Thermal Index (NTI), which satisfies all of the operational criteria imposed by the Goddard Space Flight Center (GSFC) Distributed Active Archive Center (DAAC), and allows MODIS pixels containing active lava flows to be effectively discriminated from all other pixels within the Hawaii image (Wright *et al*., 2004). According to this principle, MODVOLC triggers an alert on night-time data of the value that is more positive than -0.80. This threshold value was chosen empirically by the inspection of images containing known volcanic sites at high temperature (Wright *et al*., 2002), because it is the most negative value that avoids numerous false alarms in any region of the globe irrespective of local environmental conditions, such as the background temperature. Surfaces that are thermally homogenous at the pixel scale can be discriminated on the basis of differences in the amount of radiance they emit at 4 and 12μm. If NTI is more than -0.8 the pixel can be defined as a thermal anomaly. Using similar criteria for daytime data, and after correction for estimated solar reflection at 4μm and geometric screening to eliminate sun-glint, the MODIS thermal alert team has set a threshold of -0.60. The large swath width enables repeated night-time coverage from a single satellite to be achieved every 48 hours at the equator and at least daily at higher latitudes where orbital tracks converge. The frequency of coverage is doubled when daytime data are included (Wright, 2003; http://modis.higp. hawaii.edu/daytime.html).

METHODS AND DATA ANALYSIS

Study area

The study area focused on the hot spots detected during the 2011-2012 eruption in the volcanic field of Nyamulagira. The region shown in the Fig. 1 lies within the latitudes 1.25° to 1.50° S and within the longitudes 29.20° to 29.40° E (Fig. 1b). The study area is located in the northern part of the Nyamulagira volcano (Fig. 1.b), the western branch of the East African Rift (Fig. 1a), Virunga Volcanic Region, north of Lake Kivu (Fig. 1a), North Kivu Province (Fig. 1c) and eastern part of the DRCongo (Fig. 1d), near Rwanda.

Fig. 1: Location of the study area:
a. Map of the East African rift (Benoît et al., 2014);
b. North of Nyamulagira volcanic field (Landsat ETM + Acquired on January 26, 2010);
c. North Kivu province and d. D.R.Congo.

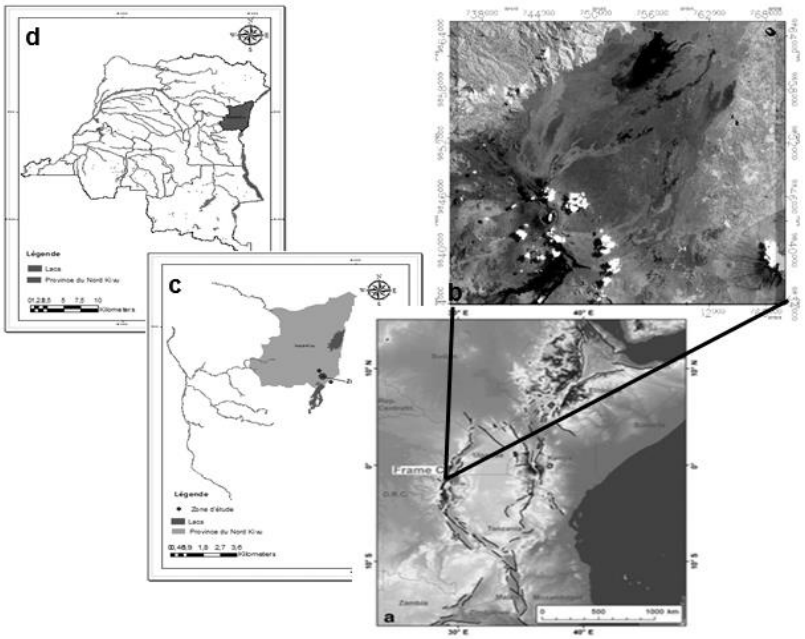

Data analysis

The MODVOLC real time data produced by the Hawaii Institute of Geophysics and Planetology, University of Hawaii at Manoa; using the Goddard DAAC software was used in this study. Data were sent every day via the internet (http://hotspot.higp.hawaii.edu/). We analyzed night-time MODVOLC data acquired and detected by the MODVOLC algorithm in the Northern part of Nyamulagira area during the period spanning between 06 November 2011 and 03April 2012. The location, radiances and the viewing geometry data were extracted in the eruptive area in order to analyze the thermal anomalies due to the occurrence of volcanic activity during the eruption. We investigated the spectral radiance at 3,960µm (21) and 12,032µm (Band 32), which are currently used for global monitoring of volcanic activity (Guéhenneux, 2010; Wright *et al*., 2004, 2003, 2002b). Using the spectral radiance at 3,960µm and 12,032µm for channels 21 and 32, we applied the Normalized Thermal Index (NTI) equation for processing to obtain the thermal anomalies detected in the eruptive area.

$$\mathbf{NTI = [Rad\ 3.9\mu m - Rad\ 12\mu m] / [R\ 3.9\mu m + Rad\ 12\mu m]}$$

(Guéhenneux *et al.,* 2010; Wright *et al.,* 2004, 2003, 2002b)

Where:
NTI = Normalized Thermal Index
Rad 3,960µm = MODIS channel 21
Rad 12µm = MODIS channel 32

NTI provides a good discrimination of active volcanic areas by a simple limit value system attached to -0.8 for the night scenes and -0.6 for the daytime scenes. Any pixel with a high NTI value is considered as a thermally anomalous target (Guéhenneux *et al.,* 2010). By analyzing the MODIS active volcanic areas in the world overnight, studies have shown that a number greater than -0.8 means a warning. Thermal anomalies in the scene with indices above -0.8 correspond to lava fountains in the crater and lava flows (Guéhenneux *et al.*, 2010).

This principle, MODVOLC triggers an alert whenever a pixel is greater than or equal to -0.8 NTI thresholds. These thresholds have been set to avoid false alarms worldwide as the overall objective of monitoring system (Guéhenneux *et al.,* 2010). To analyze the variation in time of the amount of 4µm radiance, we calculated the maximum value for the 6 November 2011 to 03 April 2012.

RESULTS

Hotspots, thermal anomalies detection, number of pixels and the maximal radiance at 4µm for all pixels alerted during the eruption.

Fig. 2: Nyamulagira 2011-2012 Eruption: Detection of hotspots (A) and NTI (B) by MODVOLC (modis.higp.hawaii.edu)

On the figure (A), the orange square represents the number of thermal events in November 2011, the chocolate square the number of thermal events in December 2011, the red square the number of thermal events in January 2012, the yellow square the number of thermal events in February 2012, the green square the number of thermal events in March 2012 and finally the blue square represents the number of thermal events in April 2012.

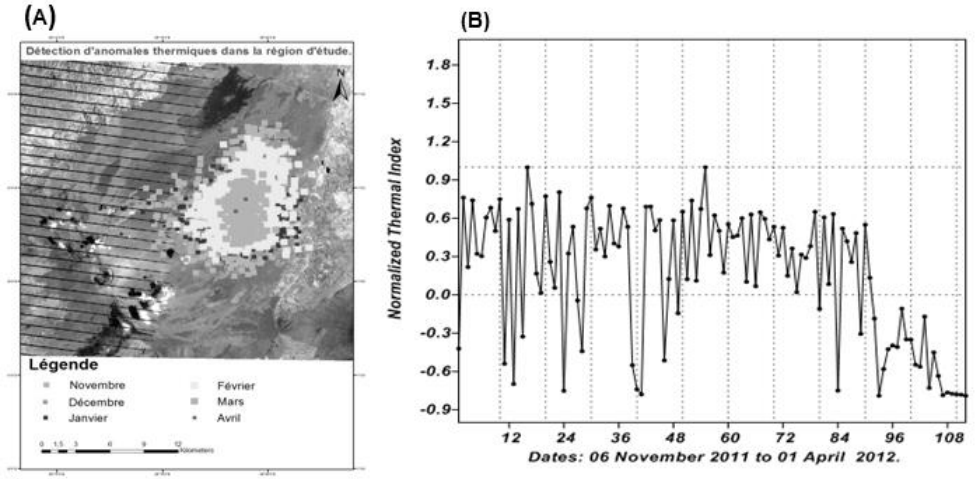

Lava flow has been detected by MODVOLC on the night of 6th November 2011 at 19:55 TU with a large thermal anomaly of 28 pixels at a resolution of 1000 m in the northern flank of the volcano. A large eruption began with a high maximum radiance amount of 90,283 W m^2 µm sr (Fig. 3B). MODVOLC proved an important development chronology of the eruption in time and space. Of the maximum radiance emitted at 4µm detected by MODVOLC, a series of six major radiance peaks were identified during several days of the

eruption on 07 November 2011 with 90,283 W m^2 µm sr; 23 November 2011 with 64,248 W m^2 µm sr; 27 November 2012 with 61,965 W m^2µm sr; 11 December 2011 with 69,471 W m^2µm sr; 18 December 2011 with 88,563 W m^2 µm sr and 01 January 2012 with 61,883 W m^2 µm sr.

MODVOLC reported a progressive decrease of the radiation at the end of the second half of March 2012 characterized by a decrease of activity of a flow with a monthly total of 226 pixels identified, this corresponds with 5.38% of pixels recorded throughout of the eruptive period. The latest hotspot was detected on 01 April 2012 (Fig. 2B) with a monthly total of 2 pixels, or 0.05% of all pixels.

Throughout the eruptive period, January and February were considered as the most abnormal from the thermal months point of view; the maximum daily frequency of pixels was reached on 01 January 2012 with a peak of 150 pixels. In total, during the eruptive period, the MODIS thermal alert algorithm flagged 4,210 pixels over the whole field of lava flows and its surrounding areas, as follows: 868 pixels in November 2011; 873 pixels in December 2011; 1,188 pixels in January 2012; 1,053 pixels in February 2012; 226 pixels in March 2012 and 3 pixels in April 2012.

Fig. 3*:* Nyamulagira 2011-2012 eruption*:***
- number of pixel (**A**) and the maximum radiance at 4 µm for all pixels alerted (**B**).

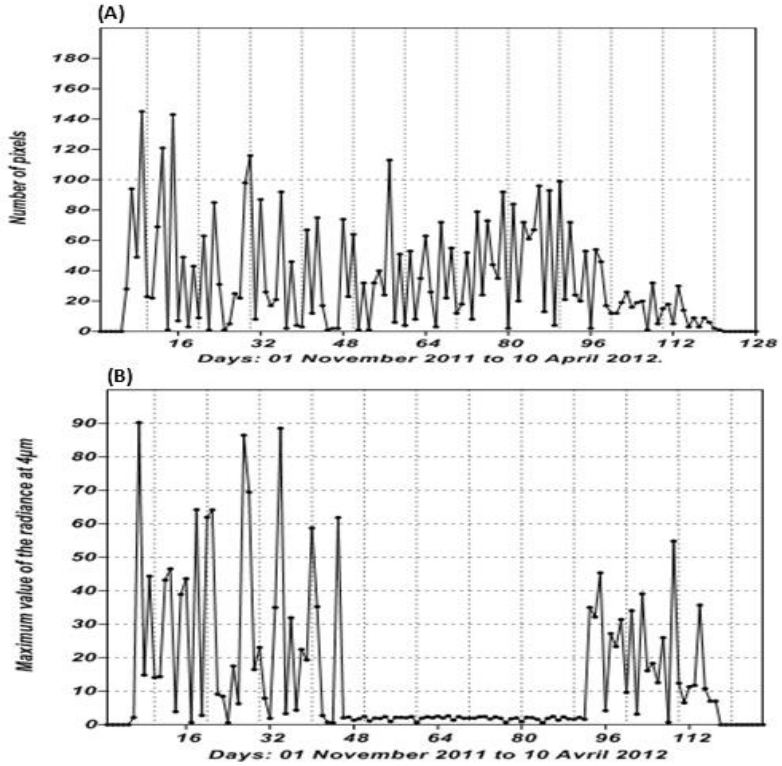

DISCUSSION

The effusive trend of the 2011–2012 eruption was characterized by a long-lasting effusive phase of high-radiating regime lasting 110 days, followed by a terminal phase of moderate-radiating regime lasting 33 days (Coppola & Cigolini, 2013). This final stage of open-vent activity was coeval with the gradual surfacing of a small thermal anomaly within the summit caldera of Nyamulagira (Coppola & Cigolini, 2013) likely associated with a shallow degassing event observed within the pit crater since April 2012 (Virunga National Park, 2012). The radiative regime peaked during the eruption and decreased when the eruptive activity became lower till the end of the eruption (Coppola & Cigolini, 2013). A transition Hawaiian Strombolian type effusive activity was frequently observed in the later stages of Nyamulagira eruption which could explain the reduction in the thermal power (Coppola & Cigolini, 2013). Between the two effusive phases, from the 1st to 48th day and the 90th to 130th day of 2011-2012 eruption (Fig. 3B), a low effusive phase of 43 days was observed, from the 48th to 90th day of the eruption, marked primarily by a lava flow.

The maximum value of thermal index was detected on 27 November 2011 with Normalized Thermal Index equal to 1 (Fig. 2B). These two months correspond with periods of large low viscosity lava.

During the eruption of Nyamulagira from November 2011 to April 2012, the MODVOLC algorithm provided a spatial and temporal chronology of the eruption. The amount of radiation detected by MODVOLC increased rapidly to a peak several days after the onset of ash. This is consistent with the common trend of large effusive eruptions resulting in the rapid increase in production levels of lava in the early eruptive stage (Wright *et al*., 2002, 2002a) before returning to a more declining phase of lava production (Wright *et al*., 2002; Harris, 2000a). However, during the 2011-2012 eruption of Nyamulagira, the descending phase was interrupted by a second increase in the thermal radiation emitted and detected by MODVOLC on 29th March 2012, with a Normalized Thermal Index of 0.042. The identification of the thermal anomalies from floating NTI allowed observing a decrease exponentially in terms of thermal energy (Fig. 2) for the last eruption on 01st April 2012 with 2 pixels only.

The distribution of hotspots reported by MODVOLC confirmed that this algorithm as a thermal data tool for monitoring eruptive events of Nyamulagira, one of the active volcanoes of the Virunga chain in particular. The application and performance of MODIS images used low spatial resolution of 1,000 m which has formed a limitation to this study. However, the temporal resolution is very high (Marzen *et al*., 2013). The threshold detection used in the automated system is also fixed, preventing customization for a better detection of specific volcanoes, where thermal activity can be more moderate. Excellent pixel location of hot-spots on the MODIS image can be confidently attributed to volcanic activity. Confusion may, however, arise when it comes to volcanoes in heavily vegetated regions as is the case of the Nyamulagira volcano if ejecting material at high temperature burned the vegetation (Ernst *et al*., 2008; Wrigth *et al*., 2003). The raw data are intact, so any thermal activity reaching the sensor would not have been missed. The weather during this time was inclement (Dehn *et al*., 2000; Nye *et al*., 2000), and the heavy clouds must have obscured the signal; however, the high level of activity in the Nyamulagira phase was often visible through clouds.

To mitigation efforts through plume monitoring and tracking, the discovery of thermal anomalies as eruption precursors marks an important step in the use of satellite remote sensing operationally to monitor remote yet dangerous volcanoes such as Nyamulagira.

CONCLUSION

The data we presented were, and will continue to be, freely available for use by our research within 24 hours of modis overpass. This paper has shown the potential of using MODVOLC data for observing and monitoring volcanic activity at Nyamulagira, how MODVOLC time-series can be used to provide useful information regarding long-lived and spatially extensive of Nyamulagira lava flows during the 2011-2012 eruption. Thermal data from weather satellites provided an otherwise unobtainable insight into eruption forerunners at Nyamulagira Volcano. During a future, longer-lasting eruption, MODVOLC will prove useful for mapping both the spatial and temporal distribution of active flows.

Based on the image chronology, and the calculated thermal anomalies for the early images, the thermal anomalies located above the summit of the Nyamulagira volcano are the signs of the magma column through the central conduit.

Although the November 2011 eruption lasted only 148 days, MODVOLC was still able to provide information regarding where lava was still flowing on the surface. The entire sequence of the 2011-2012 eruption took 4 months and 27 days, making this the longest record of thermal anomalies to a Nyamulagira event recorded by a satellite after the 1991-1993 eruption.

For Nyamulagira volcano, these data were essential to provide the warning of the impending eruption. Similarly, these remote sensing techniques are needed to monitor remote yet dangerous volcanoes in Virunga Volcanic Zone.

ACKNOWLEDGMENT

We acknowledge the NASA'TERRA (http://ltpwww.gsfc.nasa.gov/Modis/Modis.html), for providing MODIS data as well as MODVOLC for providing MODVOLC data and reviewers for providing useful comments and suggestions that greatly improved the manuscript. This research was partially financially supported by the Goma Volcano Observatory (GVO).

REFERENCES

Aoki K., Yoshida, T., Yusa, K., Nakamura, Y. (1985). Petrology and geochemistry of the Nyamuragira Volcano, Zaire. *J Volcanol Geotherm Res*, 25:1–28.

Smets, B., d'Oreye, N., Kervyn, F., Kervyn, M., Albino, F., Arellano S.R. and M. Bagalwa (2014). Detailed multidisciplinary monitoring reveals pre- and co-eruptive signals at Nyamulagira volcano (North Kivu, Democratic Republic of Congo). *Bull Volcanol*, 76:787, DOI 10.1007/s00445-013-0787-1.

Bluth, G.J.S. & Carn, S.A. (2008). Exceptional sulphur degassing from Nyamuragira volcano, 1979–2005. *Int J Remote Sens*, 29(22):6667–6685. DOI: 10.1080/ 01431160802168434.

Burt, M.L., Wadge, G., Scott, W.A. (1994). Simple stochastic modelling of the eruption history of a basaltic volcano: Nyamuragira, Zaire. *Bull Volcanol*, 56(2):87–97.

Calvari, S., Lodato, L., Steffke, A., Cristaldi, A., Harris, A.J.L., Spampinato, L., Boschi, E. (2010). The 2007 Stromboli flank eruption: chronology of the events, and effusion rate measurements from thermal images and satellite data. *J Geophys Res* 115(B4), B04201. DOI:10.1029/2009JB006478.

Chakrabarti, R., Basu, A.R., Santo, A.P., Tedesco, D., Vaselli, O. (2009). Isotopic and geochemical evidence for a heterogeneous mantle plume origin of the Virunga volcanics, Western rift, East African Rift system. *Chem Geol* 259:273–289. DOI:10.1016/ j.chemgeo.2008.11.010.

Coppola, D., Piscopo, D., Staudacher, T., Cigolini, C. (2009). Lava discharge rate and effusive pattern at Piton de la Fournaise from MODIS data. *J Volcanol Geotherm Res* 184(1–2):174–192.

Coppola, D., James, M.R., Staudacher, T., Cigolini, C. (2010). A comparison of field- and satellite-derived thermal flux at Piton de la Fournaise: implications for the calculation of lava discharge rate. *Bull Volcanol* 72(3):341–356.

Coppola, D., Piscopo, D., Laiolo, M., Cigolini, C., Delle Donne, D., Ripepe, M. (2012). Radiative heat power at Stromboli volcano during 2000–2011: twelve years of MODIS observations. *J Volcanol Geotherm Res* 215–216:48–60.

Coppola, D. & Cigolini, C. (2013). Thermal regimes and effusive trends at Nyamuragira volcano (DRC) from MODIS infrared data. *Bull Volcanol*, 75:744. DOI 10.1007/s00445-013-0744-z.

Coppola, D., Laiolo, M., Piscopo, D., Cigolini, C. (2013). Rheological control on the radiant density of active lava flows and domes. *J Volcanol Geotherm Res* 249:39–48. doi:10.1016/j.jvolgeores. 2012.09.005.

Dehn, J., Dean, K., Engle, K. (2000). Thermal monitoring of North Pacific volcanoes from space. *Geology*, 28:755–758.

Di Bartola, C., Hirn, B., Ferrucci, F., (2008). Spaceborne monitoring 2000–2005 of the Pu'uO'o-Kumaianaha (Hawaii) eruption by synergetic merge of multispectral payloads ASTER and MODIS. *IEEE T Geosci Remote Sens* 48(10):2848–2856.

Ernst, G.G.J., Kervyn,M., Teeuw, R.M. (2008).'Advances in the remote sensing of volcanic activity and hazards, with special consideration to applications in developing countries', *International Journal of Remote Sensing*, 29, 22:6687-6723.

Flynn, L. P., Harris, A. J. L., Wright R. (2001). Improved identification of volcanic features using Landsat 7 ETM+. *Remote Sensing of Environment*, 79:1 – 14.

Flynn, L. P., Wright, R., Garbeil, H., Harris, A. J. L., Pilger, E. (2002). A global thermal alert using MODIS: initial results from 2000 – 2001, *Advances in Environmental Monitoring and Modeling*, 2002, 1, 5– 36.

Gouhier, M., & Coppola, D. (2011). Satellite-based evidence for a large hydrothermal system at Piton de la Fournaise volcano (Reunion Island). *Geophys Res Lett* 38 (L02302). DOI:10.1029/2010GL046183.

Guéhenneux, Y., Labazuy, P., Bergès, J.C., Cacault, P., Souriot, T. (2010). *Observation, surveillance et alerte temps réel de l'activité des volcans par télédétection des points chauds et des panaches de cendres.* Les satellites grands champ pour le suivi de l'environnement, des ressources naturelles et des risques, Clermont-Ferrand: France, pp.1-4.

GVNW (2001d). Soufriere hills. *Bulletin of the Global Volcanism Network*, 26 (2):7 – 9.

Hamaguchi, H. & Zana N. (1983) Introduction to volcanoes Nyiragongo and Nyamuragira. In: *Hamaguchi H (ed.) Volcanoes Nyiragongo and Nyamuragira: geophysical aspects*. (pp 1–6). Tohoku University, Sendai.

Harris, A. J. L., Murray, J.B., Aries, S.E., Davies, M.A., Flynn, L.P., Wooster, M.J., Wright, R. and Rothery, D.A. (2000a). Effusion rate trends at Etna and Krafla and their implication for eruptive mechanisms. *Journal of Volcanology and Geothermal Research*, 102:237– 270, Washington, DC.

Harris, A.J.L., Flynn, L.P., Dean, K., Pilger, E., Wooster, M., Okubo, C., Mouginis-Mark, P., Garbeil, H., Thornber, C., De La Cruz-Reyna, S., Rothery, D., Wright, R. (2000). Real-time monitoring of volcanic hotspots with satellites. In P. J. Mouginis-Mark, J. A. Crisp and J. H. Fink (Eds.), *Remote sensing of active volcanism*. *American Geophysical Union Monograph: Vol.,* 116:139– 159, Washington, DC.

Harris, A.J.L., Blake, S., Rothery, D.A. and Stevens, N.F. (1997). A chronology of the 1991 to 1993 Etna eruption using advanced very high resolution radiometer data: implications for real-time thermal volcano monitoring, *Journal of Geophysical Research*, 102:7985– 8003.

Harris, A.J.L., Steffke, A., Calvari, S., Spampinato, L. (2011). Thirty years of satellite-derived lava discharge rates at Etna: implications for steady volumetric output. *J.Geophys Res* 116 (B08204). DOI:10.1029/2011JB008237. Retrieved November 10, 2011, from http://modis.higp.hawaii.edu/ daytime.html.

Hayashi, S., Kasahara, M., Tanaka, K., Hamaguchi, H., Zana, N. (1992). Major element chemistry of recent eruptive products from Nyamuragira volcano, Africa (1976–1989). *Tectonophysics*, 209:273–276.

Head, E.M., Shaw, A.M., Wallace, P.J, Sims, K.W.W., Carn, S.A. (2012). Insight into volatile behavior at Nyamuragira volcano (D.R. Congo, Africa) through olivine-hosted melt inclusions. *Geochem Geophys Geosyst*, 12:Q0AB11.

Head, E.M., Maclean, A.L., Carn, S.A. (2012). Mapping lava flows from Nyamuragira volcano, 1967–2011. With satellite data and automated classification methods. *Geomatics Nat Hazards Risk*, 2012, 4(2):119–144. DOI:10.1080/19475705.2012.680503.

Koeppen, W.C., Patrick, M., Orr, T., Sutton, J., Dow, D., Wright, R. (2013). Constraints on the partitioning of Kilauea's lavas between surface and tubed flows, estimated from infrared satellite data, sulfur dioxide flux measurements, and field observations. *Bull Volcanol* 75:216. DOI:10.1007/s00445-010716-3.

Marzen, L.J. (2013). Implications of management strategies and vegetation change in the Mount St. Helens blast zone, *Geocarto International*, 2013, 26, 5, 359-376.

Mavonga, T., Kavotha, S.K., Lukaya, N., Etoy, O., Wafula, M., Rusangiza, K.B. and Durieux, J. (2010). Some aspect of Seismicity prior the 27 November 2006 eruption of Nyamuragira volcano and it's implication for volcano monitoring and risk mitigation in the Virunga area, Western Rift Valley of Africa. *Journal of African Earth Sciences*, 58:829-832.

Nye, C.J., Keith, T.E.C., Eichelberger, J.C., Miller, T.P., McNutt, S.R., Moran, S.C., Schneider, D.J., Dehn, J., Schaefer, J.R. (2002) The 1999 eruption of Shishaldin Volcano, Alaska: monitoring a distant eruption. *Bull Volcanol*, DOI 10.1007/s00445-002-0225-2.

Piscopo, D., Coppola, D., Delle Donne, D., Cigolini, C. and Di Martino, M. (2008). Thermal anomalies at Stromboli volcano from MODIS data. *S.A.It. Suppl.Vol*.12,60.

Pouclet, A. (1975). *Activités du volcan Nyamulagira (Rift Ouest de l'Afrique Centrale), évaluation des volumes de matériaux émis. Lab*. de Volcanologie, Fac. Des sciences, Univ. de Paris-Sud, 91405 Orsay, et Dept de Géologie, E.D.S., Univ. du Bénin Lomé, Togo.

Ripepe, M., Marchetti, E., Ulivieri, G., Harris, A.J.L., Dehn, J., Burton, M.R., Caltabiano, T., Salerno, G.G. (2005). Effusive to explosive transition during the 2003 eruption of Stromboli volcano. *Geology* 33:341–344.

Rothery, D.A., Coppola, D., Saunders, C., (2005). *Analysis of volcanic activity patterns using MODIS thermal alerts*, 67:539–556.

Smets, B., Wauthier, C., d'Oreye, N. (2010). A new map of the lava flow field of Nyamulagira (D.R. Congo) from satellite imagery, *Journal of African Earth Sciences*.

Smithsonian Institution, Nyamuragira, Weekly Reports. (2011). Retrieved November 10, 2011, from http://www.volcano.si.edu/world/volcano.cfm?vnum=0203-02=&volpage= weekly#.

Steffke, A. M., Harris, A. J. L., Burton, M., Caltabiano, T., Salerno, G. G. (2011). Coupled use of COSPEC and satellite measurements to define the volumetric balance during effusive eruptions at Etna, Italy. *J Volcanol Geotherm Res* 205:45–53. DOI:10.1016/j.jvolgeores. 2010.06.004.

Toombs, A., Wadge, G. (2012). Co-eruptive and inter-eruptive surface deformation measured by satellite radar interferometry at Nyamuragira volcano, D.R. Congo, 1996 to 2010. *J Volcanol Geotherm Res* 245–246:98–122.

Ueki, S. (1983). Recent volcanism of Nyamulagira and Nyiragongo. In: Hamaguchi H (ed) *Volcanoes Nyiragongo and Nyamuragira: geophysical aspects*, (pp 7–18). Faculty of Science, Tohoku University, Sendai.

Villeneuve, M., (1980). *La structure du Rift Africain dans la Région du lac Kivu (Zaïre Oriental).* Laboratoire associé au CNRS-n.132 « Etudes géologiques ouest-africaines », Faculté des Sciences et Techniques St Jerôme, 13397, Marseille. Cedex.4.

Virunga National Park (2012). Retrieved November 10, 2013, from http://www.virunga. si.edu /nationa park/cfm?vnum.

Wadge, G. & Burt L, (2011), Stress field control of eruption dynamics at a rift volcano: Nyamuragira, D.R. Congo. *J Volcanol Geotherm Res*, 207:1–15.

Wooster, M. J. & Rothery, D. A. (2001). *A review of volcano surveillance applications using ATSR instrument series.* Advances in Environmental Monitoring and Modeling.

Wright, R. & Flynn, L. P. (2003) Satellite observations of Thermal emission before, during and after the January 2002 eruption of Nyiragongo, *Acta Vulcanolgica*, Vol.14 (1-2), 2002-15 (1-2), 2003: 67-74.

Wright, R., Flynn, L. P., Garbeil, H., Harris, A. J. L., Pilger E. (2002a). Automated volcanic eruption detection using MODIS. *Remote Sensing of Environment*, 82:135–155.

Wright, R. & Flynn, L. P. (2004). Space-based estimate of the volcanic heat flux into the atmosphere during 2001 and 2002, *Geology*, 32(3):189–192.

Wright, R., Flynn, L. P., Garbeil, H., Harris, A. J. L., Pilger, E. (2002). *Automated volcanic eruption detection using MODIS*. Hawaii Institute of Geophysics and Planetology, University of Hawaii, Honolulu, HI, USA.

Wright, R., Flynn, L. P., Garbeil, H., Harris, A. J. L., Pilger, E. (2002). MODVOLC: near-real-time thermal monitoring of global volcanism. *Journal of Volcanology and Geothermal Research* 135: 29-49.

Wright, R., & Pilger, E. (2008). Radiant flux from Earth's sub-aerially erupting volcanoes. *Int J Remote Sens* 29(22):6443–6466. DOI:10.1080/01431160802168210.

APPENDIX

Table A1: Frequency of the pixels recorded during the 2011-2012 eruption of Nyamulagira.

Date	Number of pixels	Date	Number of pixels	Date	Number of pixels
06 November 2011	28	16 December 2011	21	17 January 2012	63
07 November 2011	94	18 December 2011	92	19 January 2012	26
09 November 2011	49	19 December 2011	2	20 January 2012	3
11 November 2011	145	20 December 2011	46	21 January 2012	72
12 November 2011	23	21 December 2011	4	22 January 2012	22
13 November 2011	22	22 December 2011	3	23 January 2012	55
14 November 2011	69	23 December 2011	67	24 January 2012	12
16 November 2011	121	24 December 2011	12	25 January 2012	18
17 November 2011	1	25 December 2011	75	26 January 2012	52
18 November 2011	143	27 December 2011	17	27 January 2012	8
20 November 2011	7	28 December 2011	1	28 January 2012	79
21 November 2011	49	29 December 2011	2	29 January 2012	24
22 November 2011	3	31 December 2011	2	30 January 2012	73
23 November 2011	43	01 January 2012	74	31 January 2012	44
25 November 2011	9	02 January 2012	23	01 February 2012	35
27 November 2011	63	03 January 2012	64	02 February 2012	92
28 November 2011	1	04 January 2012	1	03 February 2012	2
02 December 2011	85	05 January 2012	32	04 February 2012	84
04 December 2011	31	06 January 2012	1	05 February 2012	20
05 December 2011	1	07 January 2012	32	06 February 2012	72
06 December 2011	5	08 January 2012	40	07 February 2012	61
07 December 2011	25	09 January 2012	24	08 February 2012	67
08 December 2011	22	10 January 2012	113	09 February 2012	96
09 December 2011	98	11 January 2012	6	10 February 2012	13
11 December 2011	116	12 January 2012	51	11 February 2012	93
12 December 2011	8	13 January 2012	4	12 February 2012	4
13 December 2011	87	14 January 2012	53	13 February 2012	99
14 December 2011	26	15 January 2012	8	14 February 2012	21
15 December 2011	17	16 January 2012	35	15 February 2012	72
16 February 2012	24	02 March 2012	26	14 March 2012	30
17 February 2012	20	03 March 2012	16	16 March 2012	14
20 February 2012	53	05 March 2012	19	18 March 2012	3
21 February 2012	2	07 March 2012	20	19 March 2012	9
22 February 2012	54	08 March 2012	1	21 March 2012	3
24 February 2012	46	09 March 2012	32	23 March 2012	9

Table A1: Continued

Date	Number of pixels	Date	Number of pixels	Date	Number of pixels
25 February 2012	17	10 March 2012	5	28 March 2012	6
26 February 2012	12	11 March 2012	15	01 April 2012	2
27 February 2012	12	12 March 2012	18	03 April 2012	1
29 February 2012	19	13 March 2012	5		

Table A2: Maximum of radiance at 4µm (MODIS band21) recorded during the 2011-2012 eruption of Nyamulagira

Date	Max.Rad.at 4µm	Date	Max.Rad.at 4µm	Date	Max.Rad.at 4µm
06 November 2011	2.146	16 December 2011	35.024	21 January 2012	2.4
07 November 2011	90.283	18 December 2011	88.563	22 January 2012	0.663
09 November 2011	14.839	19 December 2011	3.293	23 January 2012	1.978
11 November 2011	44.353	20 December 2011	31.969	24 January 2012	2.369
12 November 2011	14.105	21 December 2011	4.348	25 January 2012	2.093
13 November 2011	14.368	22 December 2011	22.505	26 January 2012	2.543
14 November 2011	43.213	23 December 2011	-	27 January 2012	2.023
16 November 2011	46.564	24 December 2011	19.368	28 January 2012	2.653
17 November 2011	3.902	25 December 2011	58.779	29 January 2012	1.378
18 November 2011	38.929	27 December 2011	35.282	30 January 2012	2.44
20 November 2011	43.644	28 December 2011	2.761	31 January 2012	1.943
21 November 2011	-	29 December 2011	0.75	01 February 2012	2.009
22 November 2011	0.697	31 December 2011	0.615	02 February 2012	1.978
23 November 2011	64.248	01 January 2012	61.883	03 February 2012	2.184
25 November 2011	2.792	02 January 2012	2.071	04 February 2012	2.39
27 November 2011	61.965	03 January 2012	2.276	05 February 2012	2.416
28 November 2011	-	04 January 2012	-	06 February 2012	2.442
02 December 2011	64.188	05 January 2012	1.343	07 February 2012	1.715
04 December 2011	9.13	06 January 2012	1.572	08 February 2012	2.341
05 December 2011	8.486	07 January 2012	1.801	09 February 2012	1.939
06 December 2011	0.615	08 January 2012	2.491	10 February 2012	0.694
07 December 2011	17.538	09 January 2012	1.107	11 February 2012	1.768
08 December 2011	6.281	10 January 2012	1.981	12 February 2012	1.901
09 December 2011	86.48	11 January 2012	1.934	13 February 2012	2.033
11 December 2011	69.471	12 January 2012	1.887	14 February 2012	0.896
12 December 2011	16.524	13 January 2012	2.149	15 February 2012	2.186
13 December 2011	23.059	14 January 2012	2.411	16 February 2012	2.113
14 December 2011	7.925	15 January 2012	0.996	17 February 2012	1.623

Table A2: Continued

Date	Max.Rad.at 4µm	Date	Max.Rad.at 4µm	Date	Max.Rad.at 4µm
15 December 2011	1.929	16 January 2012	2.192	18 February 2012	0.615
16 February 2012	35.024	17 January 2012	2.175	19 February 2012	-
17 February 2012	88.563	18 January 2012	-	20 February 2012	1.905
19 February 2012	3.293	19 January 2012	2.082	21 February 2012	2.188
20 February 2012	31.969	20 January 2012	2.241	22 February 2012	2.471
23 February 2012	1.378	08 March 2012	27.217	22 March 2012	-
24 February 2012	2.352	09 March 2012	23.358	23 March 2012	12.42
25 February 2012	1.749	10 March 2012	31.44	24 March 2012	-
26 February 2012	1.652	11 March 2012	9.653	25 March 2012	6.54
27 February 2012	2.172	12 March 2012	34.081	26 Mars 2012	11.34
28 February 2012	-	13 March 2012	3.17	27 Mars 2012	11.751
29 February 2012	1.639	14 Mars 2012	39.101	28 Mars 2012	35.752
01 Mars 2012	-	15 March 2012	-	29 Mars 2012	-
02 Mars 2012	35.059	16 Mars 2012	16.116	30 Mars 2012	10.757
03 Mars 2012	32.205	17 Mars 2012	18.338	31 Mars 2012	-
04 Mars 2012	-	18 Mars 2012	12.562	01 April 2012	25.982
05 Mars 2012	45.379	19 Mars 2012	26.013	02 April 2012	-
06 Mars 2012	-	20 Mars 2012	0.736	03 April 2012	7.063
07 Mars 2012	4.179	21 Mars 2012	54.844	04 April 2012	-

Table A3: Normalized Thermal Index during the 2011-2012 eruption of Nyamulagira

Date	NTI	Date	NTI	Date	NTI
06 November 2011	-0.42	13 December 2011	0.535	08 January 2012	0.585
07 November 2011	0.763	14 December 2011	-0.043	09 January 2012	-0.143
09 November 2011	0.219	15 December 2011	-0.441	10 January 2012	0.653
11 November 2011	0.742	16 December 2011	0.679	11 January 2012	0.123
12 November 2011	0.323	17 December 2011	-	12 January 2012	0.74
13 November 2011	0.304	18 December 2011	0.763	13 January 2012	0.112
14 November 2011	0.607	19 December 2011	0.356	14 January 2012	0.674
16 November 2011	0.684	20 December 2011	0.52	15 January 2012	1
17 November 2011	0.501	21 December 2011	0.302	16 January 2012	0.312
18 November 2011	0.751	22 December 2011	0.699	17 January 2012	0.624
20 November 2011	-0.539	23 December 2011	0.404	18 January 2012	-
21 November 2011	0.50	24 December 2011	0.38	19 January 2012	0.503
22 November 2011	-0.697	25 December 2011	0.678	20 January 2012	0.174
23 November 2011	0.674	26 December 2012	-	21 January 2012	0.555

Table A3: Continued

Date	NTI	Date	NTI	Date	NTI
25 November 2011	-0.326	27 December 2012	0.534	22 January 2012	0.454
27 November 2011	1	28 December 2012	-0.55	23 January 2012	0.465
28 November 2011	0.731	29 December 2012	-0.739	24 January 2012	0.602
02 December 2011	0.714	30 December 2012	-	25 January 2012	0.103
04 December 2011	0.168	31 December 2012	-0.778	26 January 2012	0.631
05 December 2011	0.016	01 January 2012	0.692	27 January 2012	0.069
06 December 2011	0.773	02 January 2012	0.692	28 January 2012	0.648
07 December 2011	0.259	03 January 2012	0.506	29 January 2012	0.596
08 December 2011	0.056	04 January 2012	-	30 January 2012	0.435
09 December 2011	0.806	05 January 2012	0.587	31 January 2012	0.535
11 December 2011	-0.751	06 January 2012	-0.513	01 February 2012	0.308
12 December 2011	0.325	07 January 2012	0.125	02 February 2012	0.527
03 February 2012	0.15	24 February 2012	0.135	16 March 2012	-0.634
04 February 2012	0.364	25 February 2012	-0.185	17 March 2012	-
05 February 2012	0.022	26 February 2012	-0.789	18 March 2012	-0.785
06 February 2012	0.317	27 February 2012	-0.58	19 Mars 2012	-0.764
07 February 2012	0.29	28 February 2012	-	20 Mars 2012	-
08 February 2012	0.382	29 February 2012	-0.424	21 Mars 2012	-0.774
09 February 2012	0.652	01 Mars 2012	-	22 Mars 2012	-
10 February 2012	-0.109	02 Mars 2012	-0.395	23 Mars 2012	-0.778
11 February 2012	0.608	03 March 2012	-	24 Mars 2012	-
12 February 2012	0.085	04 Mars 2012	-	25 Mars 2012	-
13 February 2012	0.634	05 Mars 2012	-0.107	26 Mars 2012	-
14 February 2012	-0.749	06 Mars 2012	-	27 Mars 2012	-
15 February 2012	0.521	07 Mars 2012	-0.348	28 Mars 2012	-0.781
16 February 2012	0.421	08 Mars 2012	-	29 Mars 2012	-
17 February 2012	0.258	09 Mars 2012	-0.35	30 Mars 2012	-
18 February 2012	-	10 Mars 2012	-0.546	31 Mars 2012	-
19 February 2012	-	11 Mars 2012	-0.562	01 April 2012	-0.789
20 February 2012	0.485	12 Mars 2012	-0.169	02 April 2012	-
21 February 2012	-0.305	13 Mars 2012	-0.728	03 April 2012	0.784
22 February 2012	0.551	14 Mars 2012	-0.449	04 April 2012	-
23 February 2012	-	15 March 2012	-	05 April 2012	-

The Normalized Thermal Index was calculated by normalizing the difference between the recorded 4 and 12 µm radiance by the sum of the 4 and 12 µm radiances (Guéhenneux 2010; Wright et al. 2004, 2003, 2002, 2002b).